

1-23-1991

Phenomena Relating to Charge in Insulators: Macroscopic Effects and Microscopic Causes

Jacques Cazaux
Faculté des Sciences

Claude Le Gressus
CEA CEN/Saclay

Follow this and additional works at: <https://digitalcommons.usu.edu/microscopy>



Part of the [Physics Commons](#)

Recommended Citation

Cazaux, Jacques and Le Gressus, Claude (1991) "Phenomena Relating to Charge in Insulators: Macroscopic Effects and Microscopic Causes," *Scanning Microscopy*. Vol. 5 : No. 1 , Article 2. Available at: <https://digitalcommons.usu.edu/microscopy/vol5/iss1/2>

This Article is brought to you for free and open access by the Western Dairy Center at DigitalCommons@USU. It has been accepted for inclusion in Scanning Microscopy by an authorized administrator of DigitalCommons@USU. For more information, please contact digitalcommons@usu.edu.



PHENOMENA RELATING TO CHARGE IN INSULATORS:
MACROSCOPIC EFFECTS AND MICROSCOPIC CAUSES

Jacques Cazaux^{1,*} and Claude Le Gressus²

¹Faculté des Sciences, BP 347, 51602 Reims Cedex, France
²CEA CEN/Saclay, DSM.SPAS, 91191 Gif-sur-Yvette Cedex, France

(Received for publication January 31, 1990, and in revised form January 23, 1991)

Abstract

Conservation of current under steady-state conditions makes it possible to determine the sign of charges trapped in an insulator subjected to ionizing radiation. The maximum value of the surface potential can thus be estimated.

On the basis of a given trapped charge distribution, the pattern of the electrical field and of the potential can thus be established, and the influence of the shape of the sample and its environment can be clearly shown. Change of trapped charges with time (at the start and after irradiation) is then examined. Finally, the microscopic causes of trapping of charge is suggested by analogy with semiconductors. Each stage is illustrated with examples and a number of practical consequences are deduced.

To facilitate the understanding of the phenomena, this analysis begins with the better known macroscopic effects and works back to microscopic causes, which are often poorly controlled. Since the inverse process would be more logical, we have mentioned it in the conclusion, while pointing out some of the difficulties which arise.

KEY WORDS : Insulator, dielectric, bombardment, flashover, electric field, electromigration.

*Address for Correspondence:

Jacques Cazaux
Laboratoire de Spectroscopie des Electrons
BP 347 Faculté des Sciences
51062 Reims Cedex, France

Phone : 33.26.05.32.23
Fax : 33.26.05.32.50

1. Introduction

Charge phenomena in insulators occur in a wide range of materials (polymers, oxides, nitrides, borides, glasses, ceramics, geological minerals, biological specimens, etc.) when they are subjected to various types of radiation, such as with electrons (in Scanning Electron Microscopy (SEM), Transmission Electron Microscopy (TEM), Scanning Transmission Electron Microscopy (STEM), and the associated Electron Probe Microanalysis (EPMA), and Auger Electron Spectroscopy (AES) analysis methods), ions in Ion Scattering Spectroscopy (ISS), Secondary Ion Mass Spectrometry (SIMS), and Proton Induced X-ray Microscopy (PIXE), as well as X-rays (in X-Ray Photoelectron Spectroscopy (XPS) and X-ray Lithography).

These phenomena result in a variety of effects such as deflection of the incident beam, migration of mobile species, energy shift of spectra (as in XPS and AES), apparent desorption of certain species, the distortion of spectra and images, flashover, and even the destruction of the specimen.

These effects depend not only on the elements entering into the composition of the specimen studied but also its crystalline state, any impurities that it may contain, its shape (thin film or thick body) its surface (metal coated or not) and its environment (grid, sample holder and detectors polarized or not). They also depend on the experimental conditions, for example the nature, the energy and the intensity of the incident beam and whether the irradiation is permanent or intermittent.

It is thus clearly impossible to cover all the different effects and to explain them in a detailed manner, or to make reference to all the hundreds if not thousands of articles describing these effects, and the numerous contradictions which they contain. Nevertheless, using as a basis the conservation of current under steady state conditions, we first estimate the sign of the trapped charges and the surface potential of a thick insulator (then a thin film) bombarded by charged particles (§ 2). Then, using basis laws of electrostatics, we give (§ 3) the pattern of the electric field created in a vacuum and in the insulator by trapped charges. Then, in § 4, we give the

List of symbols

δ	: secondary emission coefficient
η	: coefficient of back-scattering
σ	: $\delta + \eta$
I_0	: incident current
I_r	: current escaping into the vacuum
I_s	: absorbed current
U_s	: surface potential
U_0	: primary electron acceleration voltage
R	: sample leakage resistance
ϵ	: sample dielectric constant
ρ	: density of trapped charges per unit volume
E_{c1}, E_{c2}	: primary energy values of electrons for which $\sigma = 1$
T	: fraction of transmitted electrons which exit the sample through the face opposed to the irradiated face
γ	: conductivity.

variation of such trapped charges with time (at the beginning of irradiation and when the incident beam is stopped). Finally, in § 5, we consider the possible microscopic causes of trapping and untrapping of incident particles, using analogies with similar phenomena occurring in semiconductors and dielectric material discharge theory. At each stage, we illustrate our discussion with experimental examples derived from scientific literature and deduce certain practical consequences.

To facilitate the understanding of the phenomena, the reasoning begins with the macroscopic effects most frequently observed and works back to the microscopic causes, over which one has much less control. It would be more consistent to start with the microscopic causes and derive their macroscopic consequences. This last process is outlined in the conclusion, whereas the pitfalls of the method used are pointed out at the end of each section.

2. The sign of trapped charges under steady state conditions

The case of a insulator bombarded with electrons

The case which is the most complicated but also that which has been studied the most is that of the sign of the trapped charge and the potential U_s which develops at the surface (limited by the vacuum) of a thick insulator subjected to bombardment with primary electrons of intensity I_0 and energy eU_0 . In this case, under steady state conditions (i.e. when the intensity and distribution of the trapped charges no longer change), the conservation of electrical current can be written as follows :

$$I_0 = I_r + I_s \tag{1}$$

If I_0 and I_r (current escaping into the vacuum) are considered to be positive, corresponding to the direction of movement of the electrons, the sample current I_s which results from the difference between I_0 and I_r will have a sign opposite to the sign of the trapped charges and that of the surface potential. Thus if I_s is positive, the corresponding electrons escape and the

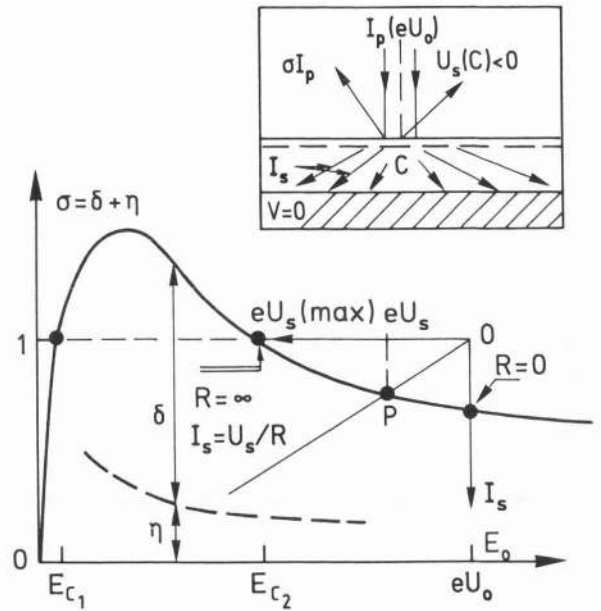


Figure 1 : Thick insulators : The effect of primary energy $E_0 = eU_0$ on total electron emission, $\sigma = \delta + \eta$, with two critical energy levels E_{c1} and E_{c2} at which $\sigma = 1$. When $eU_0 > E_{c2}$, the charges which develop at the surface are negative, the incident electron beam is slowed and the operating point moves towards E_{c2} , which it only reaches when the leak resistance, R , is infinite. The surface potential is then given by expression (2). In the case where R is finite, the operating point is P but determination of R is a delicate matter as (see inset) the current density in the specimen is not uniform. However, according to Reimer (1985), the determination of P only requires using the eU_0 and I_s coordinate system (on the right side of the figure) and straight line $I_s = U_s/R$.

electrical charge of the specimen and its surface potential will be negative.

If $I_r = \sigma I_0$, with σ being the total electron emission yield ($\sigma = \delta + \eta$ where η is the coefficient of back-scattering and δ is the secondary emission coefficient), it has been deduced (Reimer, 1985), that it is possible for the surface potential to be positive when $\sigma > 1$, i.e. when $E_{c1} < eU_0 < E_{c2}$ or negative when $\sigma < 1$, i.e. when $eU_0 > E_{c2}$.

In the case of a negative surface potential, the incident electrons are slowed by the potential (their kinetic energy is $e(U_0 + U_s)$) which results in a reduction of σ and displacement of the operating point towards the critical point E_{c2} (which, like E_{c1} , corresponds to $\sigma = 1$).

This critical point E_{c2} is only attained when conductivity γ of the insulator is null and the surface potential is then :

$$U_s(\max) = (E_{c2}/e) - U_0 \tag{2}$$

It can reach excessively high values if U_0 is high. As indicated by Reimer (1985), allowance for a non-null conductivity γ (and

hence a leak resistance R which is not infinite) in principle makes it possible to graphically evaluate U_s by intersection of the straight line $I = U/R$ with the curve $\sigma = f(E_p)$ (see figure 1). In practice, the calculation of R is an extremely delicate matter a surface of the insulator is not equipotential (U_s varies in its plane), the electric field (and the current density) in the insulator is not uniform (see inset in figure 1) which gives a value of R which differs from that of the conventional expression, $I/\gamma S$ even for a lamella with parallel sides of homogeneous thickness l and area S . This also results in highly complex equations derived from solving the Laplace equation when the analysis of a real case is envisaged (presence of grids on the surface or metal parts in the vicinity).

The result of the analysis is that it is only possible to estimate -with the aid of expression (2)- the upper limit which can be reached or to measure U_s experimentally by the shift in the spectrum of the secondary electrons and the Auger electrons.

When the primary energy is such that $E_{c1} < eU < E_{c2}$, the specimen becomes positively charged, the primary electrons are thus accelerated in its vicinity so that, for infinite leak resistance, the point of equilibrium moves towards E_{c2} . Nevertheless, in this case, in the absence of an external electrode placed at its positive potential (see Brunner and Schmid, 1986, for a detailed study of these effects) or a specimen holder placed at a negative potential of a nature to facilitate extraction of the secondary electrons, electrons with a kinetic energy of less than eU cannot escape or return to the surface, which results in a drop in secondary emission σ and a surface potential of a few volts at the most. This analysis is shown in figure 2.

Allowance for specimen current I_s does not significantly change the situation. The surface potential could be deduced from expression (1), which becomes :

$$I_0 - I_0 \int_{eU_s}^{\infty} \left(\frac{\partial \delta}{\partial E} + \frac{\partial \eta}{\partial E} \right) dE = U_s/R \quad (3)$$

provided the expression is known which gives the spectral distribution of the secondary and backscattered electrons as a function of their kinetic energy E (and knowing their dependence as a function of eU_0).

The case of a thin film bombarded with electrons

If the insulator specimen, in the form of an unsupported thin film, is bounded by a vacuum on both sides, it is easy to establish the sign of its surface potential by allowing, in current conservation, for the intensity of the primary current escaping $T \cdot I_0$ and the increased secondary emission δ'_1 by the contribution of the opposite side δ'_2 (symbols ' in δ' and, further, η' suggest that coefficient in thin films are different from those in thick samples. Niedrig, 1982). If T is the film transmission coefficient, the following expression is

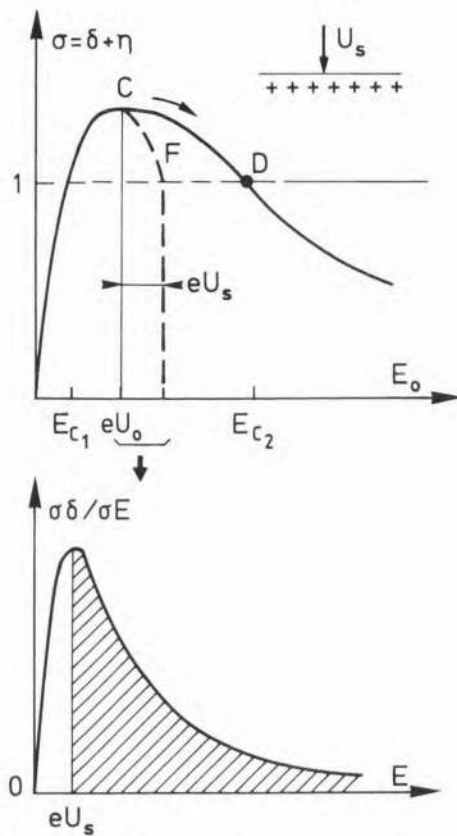


Figure 2 : Thick insulators : Primary energy eU is such that $E_{c1} < eU < E_{c2}$. The surface potential is positive and accelerates the incident electrons, resulting in (upper curve) a shift in the operating point from C towards D . But this positive potential reduces secondary electron emission (lower curve) so that the operating point moves from C to F , limiting the surface potential to $U_s = (E_F/e) - U_0$.

obtained :

$$(1-T) = (\delta'_1 + \delta'_2 + \eta') + (I_s/I_0) \quad (4)$$

This results in a positive potential even when E_0 is such that $E_0 \gg E_{c2}$ (thick material) if the thickness of the film is well below the penetration depth, R_e , of incident electrons in the same material when thick. This is the case, in particular, in transmission electron microscopy (TEM and STEM) where $E_0 = 100$ keV or the thickness (~ 100 nm) are such that $t \ll R_e$, while remaining greater than the escape depth of the secondary electrons (Cazaux, 1986a).

The self-regulation corresponding to the reduction in secondary emission (when U_s increases), should play its role (except in the presence of disturbance causes by exterior electric or magnetic fields). Nevertheless, compared to the situation shown in figure 2, the level of this self-regulation depends on the thickness of the film (which affects T , δ_2 and to a lesser degree η) but in films which are

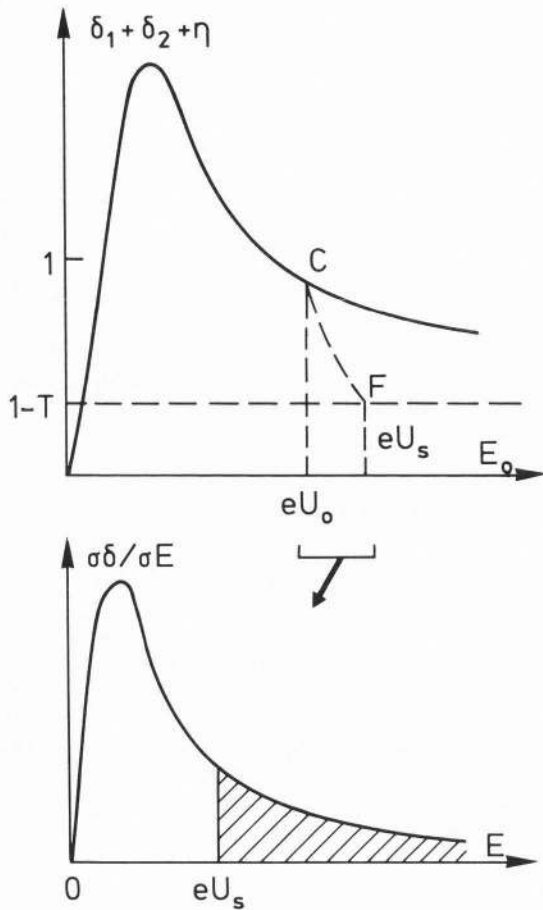


Figure 3 : In the case of an unsupported film, secondary emission as a function of primary energy is greater (relative to the situations in figures 1 and 2) whereas the equilibrium reference point becomes $1 - T$ and no longer 1 (upper figure). Even at relatively high primary energies, the charge of the specimen will remain positive. Nevertheless, the surface potential will be limited to a few tens of volts or less due to the reduced secondary emission by self-regulation (see lower curve).

sufficiently thin it can reach a relatively high level (U_s ten volts or more) as shown in figure 3. An analysis of the same type, and, in some respects, more thorough, was performed for the first time by Hobbs (1974), also see Hobbs, 1990 (in this volume). It leads to the same qualitative conclusions.

In the case where the insulating film is deposited on a conducting substrate (for example SiO_2 on doped Si) and is observed with a scanning electron microscope (SEM), the result is an equation analogue to expression 4, where T is the primary current transmitted in the substrate and I_s is the current escaping from the insulator, which makes it difficult to measure separately as it adds to the contribution TI_0 . Relative to the unsupported film situation, the fact that δ_2 is null limits the range of the values of E_0 inducing positive surface potential and charges, the range

nevertheless being greater than (E_{c1}, E_{c2}) of the insulating material in the thick condition. The energy inversion value E_{c2} (overlayer) depends on the thickness of the film and increases as the film becomes thinner. Instead of determining the current balance, it is possible to qualitatively express the sign of the trapped charges by evaluating their algebraic sum, allowing for the positive charges Q_+ resulting from desorption of the secondary electrons over thickness d ($d < 50 \text{ nm}$) and the negative charges Q_- resulting from trapping of the incident electrons in thickness t of the thin film or d_1 of the thick material where d_1 is approximately equal to $1 \mu\text{m}$ (Cazaux, 1986a).^P

The case of irradiation by other particles

The approach described above can be applied to other incident particles.

In the case of irradiation of the insulator with neutral particles (metastable atoms or photons), the contribution of incident current I_0 and back-scattered current η is null in the expression (1), (3) and (4).

All that remains is secondary electron emission compensated by the specimen current: the surface potential and the trapped charges are naturally positive. As there is no negative charge, the self-regulation of the potential can only take place via resistance leakage.

Thus, in XPS, expression (3) can be reduced as follows:

$$N_0 \cdot e \int_{eU_s}^{\infty} \frac{\partial \delta}{\partial E} dE = - U_s / R \quad (5)$$

where N_0 = the number of incident photons per second.

A similar analysis could be made in the case of bombardment by protons, adding the contribution of the primary beam with reinforces the positive nature of the charge (see Schou, 1988, for secondary electron emission).

We shall not be considering the case of incident ions as although it is possible to evaluate the surface potential sign, detailed analysis is complicated by its permanent change under ionic erosion.

Practical consequences

The charging effects of the insulators result in disturbances in their examination with electron microscope, for instance.

In SEM, it is frequently recommended that one select a primary energy value which is equal to critical energy E_{c2} , to provide freedom from these effects; but, as observed by Brunner and Schmid (1986), in heterogeneous materials, secondary emission varies from one component to another, making it impossible to maintain an equilibrium between the incident current and the currents emitted by the surface as a whole. Even for a material of homogeneous composition, topographic effects locally change the secondary emission as δ depends on the local angle of incidence (causing contrast in SEM). Consequently, it is only in Auger spectroscopy of specimens, which are perfectly flat and homogeneous in composition, that such measures

are effective. The choice of a level energy E_0 such that $E_{c1} < E_0 < E_{c2}$ offers the advantage of inducing a positive surface potential which does not repel incident beam. Nevertheless, as local secondary emission will vary from one point to another, it will induce local variations of surface potential and the corresponding electrical lines of force will act as an equivalent number of electrostatic lenses, resulting in distortion of the electronic images in SEM. Brunner and Schmid (1986) observe that this local shift may be less than the resolution of the microscope ($<0.1 \mu\text{m}$) in SEM (between E_{c1} and E_{c2}).

In a negative charge state, the addition of an auxiliary neutralization gun also makes it possible to introduce local compensation for charging effects but this compensation cannot be perfect, particularly in depth, as penetration of the primary electrons is greater than that of the neutralization electrons. Nevertheless, in a positive charge state, such as in XPS, the addition of an auxiliary gun has been found to be effective (Barth et al., 1988). In a similar field, one should also mention the outstanding contribution by Liehr et al. (1986).

Finally, the method developed in EPMA consists of depositing metal on the surface of the specimen to be analysed. We shall see in the following section that although this procedure facilitates analysis as it stops deflection of the incident beam outside the specimen, it modifies the electric field inside the specimen without stopping it. It could be used for the observation of insulators in TEM provided the conductive layers on the two sides of the specimen are perfectly continuous, it being borne in mind that it will consequently be able to cause image distortion and reduce resolution. To conclude concerning this point, it is possible, like Werner and Warwoltz (1984), to take the point of view that although these effects cannot be completely prevented, procedures are available to minimize them.

Critical analysis

The investigation described in this section is based on a relationship of dependence between secondary emission and primary energy which is the same as in metals (figures 1 to 3). Experimental data on insulators are few, because of the experimentation difficulties created by the interference of charge effects with the phenomenon under investigation (self-regulation as illustrated by figure 2).

In the case of single-crystal MgO (001), the secondary emission coefficient could be in excess of 20 (Whetten and Laponski, 1959). This could be explained by the fact that secondary electrons in insulators have an escape depth which is far in excess of that in metals, since such electrons are not subject to electron-electron interactions with conduction band electrons (as they would be in the case of metals). Thus, the mean free path of electrons with 10 eV kinetic energy can reach 100 nm in alkali halides (Hobbs, 1974). This depth is typical of the samples subjected to transmission-type electron microscopy, and enhances the positive character of the charge they acquire, even when bombarded with 100 keV

electrons. It is therefore essential to obtain more experimental data on the secondary emission of insulators, as a function not only of their chemical composition, but also of their crystalline condition and imperfections.

The second remark relates to equations (3) and (5) of figure 1, which suggest a relationship of the ohmic type between surface potential U_s and sample current I_s , i.e., $U_s = RI_s$. This reasoning implies disregarding local variations in conductivity due to electronic bombardment and to the electric field created by the trapped charges (Hobbs, 1974). Mainly, it makes no distinction between the electrons injected into the insulator by electronic bombardment and the conduction electrons of that same insulator in the absence of bombardment. Experimental evidence of non-ohmic behaviour was given by Moëller and He (1986), who observed that MgO in single-crystal form was not becoming charged under certain conditions ($U_s = 0$), when equilibrium between I_s and I_r had probably not been reached ($I_r \neq 0$). It follows, somewhat paradoxically, that the resistance of this insulator is null under electron bombardment conditions. An explanation for this phenomenon is given in section 5.

3. Distribution of the electric field at the surface and inside insulators

Properties of the electric field induced

One consequence of bombardment of an insulator with a beam of charged particles is the appearance of a trapped charge pattern, $\rho(r,z)$, using cylindrical coordinates for normal incidents.

If this charge pattern is known, it is in principle possible, using the laws of electrostatics, to calculate the electric field $F(r,z)$ and the potential $V(r,z)$. Even if this pattern is not exactly known, these laws nevertheless make it possible to obtain certain information concerning F .

Thus, in the case of an infinite medium, the field created by a charge pattern is either centrifugal or centripetal (depending on the sign of the charges) and that it changes in direction along any straight line through charge pattern centre C, where F is canceled out before changing direction.

F can in no case be uniform (and the potential constant) as, using the Gauss theorem,

$$\text{div } F = \rho/\epsilon \neq 0 \quad (6)$$

where ϵ is the dielectric constant of the insulator. When the insulator in the form of a lamella with parallel surfaces bonded by two media of dielectric constant ϵ_1 and ϵ_2 , it is possible to evaluate field F_1 in this insulator using the electrical image theory. This field results not only from the fields created by the actual charges, ρ , but also the fields created by image charges deduced from the real charge by symmetry relative to the interfaces and a combination of the two. The weight of these two images is $K_1\rho$ and $K_2\rho$ with :

$$K_1 = \frac{\epsilon - \epsilon_1}{\epsilon + \epsilon_1} \quad \text{and} \quad K_2 = \frac{\epsilon - \epsilon_2}{\epsilon + \epsilon_2} \quad (7 \text{ and } 7')$$

The weight can be either positive or negative. It is, in particular, negative when the surrounding medium is conductor ($\epsilon_1 = \infty$ hence $K_1 = -1$).

The effect of image electric charges accounts for the fact that, for a given distribution of actual charges, the electric field in the insulator is dependent on the thickness of the sample and on its environment. For a thin film in vacuum the field will be mainly radial and its axial component will increase when the thickness of the film increases. For a thick sample the axial component will be maximum at the end of the real charge distribution when the surface of the sample is in contact with vacuum; the axial component of the field will be maximum at the surface in the case of an insulator coated with metal (Cazaux, 1986a and b).

The electrical image theory makes it possible to not only estimate the influence of the nature of the surrounding media on the electric field and the potential in the insulator, and the influence of its thickness, but also the experimental conditions concerning focussed or defocussed irradiation (Cazaux, 1986b).

In particular, it shows that the surface potential cannot be constant except in the case of a metal coated interface (Cazaux, 1986c), and that the field is never uniform but that it changes in direction along a line between the two interfaces.

Practical consequences

This analysis has made it possible to explain a number of well-known phenomena for the first time.

For example, the radial field explains the radial stresses to which unsupported insulating films are subjected when observed using a TEM (Cazaux, 1988). In the same way, considering electrostatic pressure effects, the fact that the electrostatic field has a maximum value at the metal-dielectric interface (in a direction normal to the interface), explains the increased adherence of conducting films covering an insulator when irradiated by a beam of charged particles.

Above all, it explains the variation with time of signals (EPMA, AES, etc.) relating to mobile ions in insulators (such as glasses) when irradiated. Indeed, due to the electric field created by the trapped charges, the Coulomb force acts on the mobile ions, which, according to their sign, will then accumulate in the zone of interest, or move away from it. Figure 4 (from M. Tencé et al., 1989) illustrates the decrease in the X-ray emission signal of sodium during irradiation with electrons. This electromigration is the fingerprint of the electrical field established in the insulator.

For example, figure 5 compares the sodium ion diffusion profile obtained by SIMS after irradiation of a glass with a 600 keV proton beam (Battaglin et al., 1982) with distribution of the electric field as a function of the depth in the insulator, of which the surface was metal coated. As in figure 6, the experimental profile

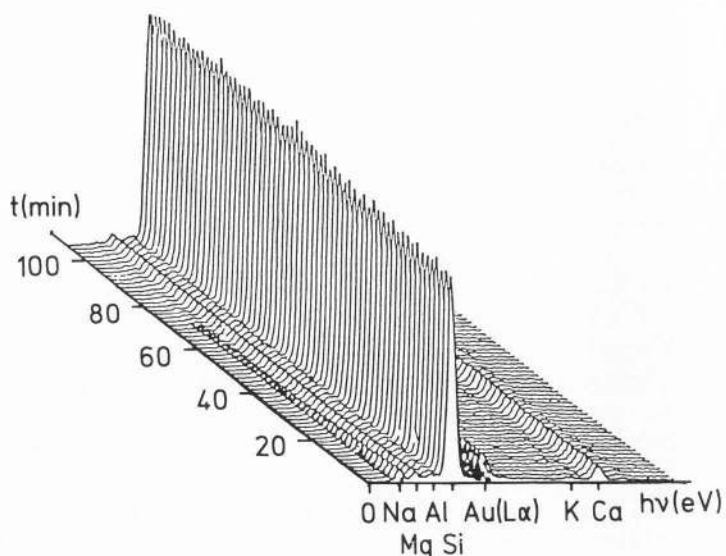


Figure 4 : Change with time of the X-ray emission spectrum of a glass bombarded with a 20 keV electron beam. The glass is covered with a film of gold to prevent charging effects and, at regular intervals, the entire X-ray spectrum is acquired simultaneously with a Si(Li) detector. Particularly note worthy is the decrease in the sodium signal and the slight increase in the silicon signal.

of distribution of the sodium ions in the vacuum/glass/metal system (Ohuchi et al., 1980) is compatible with the calculated change of F_z as a function of depth.

Critical analysis

The difficulty of this approach is that it necessitates knowledge of distribution $\rho(r,z)$ of the trapped charges. If the distribution is known, it is theoretically possible to calculate the electric field thus created through correct application of the laws of electrostatics.

Unfortunately, the evaluation of $\rho(r,z)$ presents two difficulties :

- i) an inadequate knowledge of the electric charge entrapment process ; and
- ii) time-dependent charge variations.

As regards the first problem, the incidence of the sample crystalline state and imperfections would need clarification. We feel that crystal imperfections play a decisive role and that two crystalline varieties of one sample (mono- and polycrystalline) yield different distribution of trapped charges, and therefore induced electric fields which are different even if the geometry of the sample, and experimental conditions are identical. Thus, in thin films of α single-crystal alumina, irradiated by a narrow electron beam, trapped charges would be located close to the dielectric/vacuum interfaces; the electric field thus created would be normal to the interfaces, and located at the centre of the irradiated zone (case of uniformly charged, plane discs). In the case of the same alumina film, but with a polycrystalline structure, and

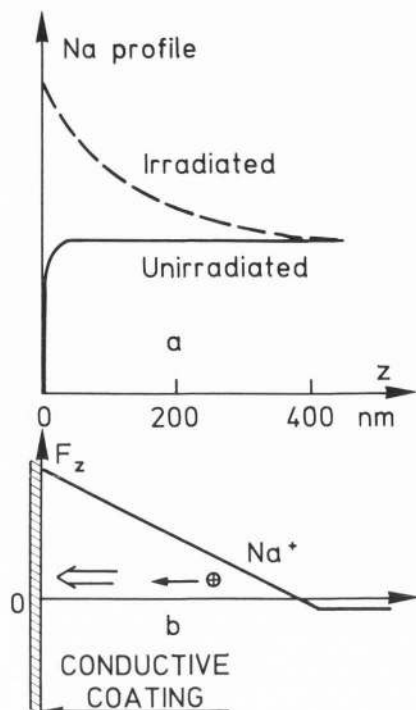


Figure 5 : Comparison between the experimental profile of sodium obtained in a glass covered with a conducting film irradiated with protons (top) with the calculated change of the electric field induced by a strongly defocalized positive charge distribution (bottom).

uniform distribution of imperfections though the volume, the distribution of trapped charges would also be more or less uniform through the volume, and the electric field thus created would be that of a long, thin cylinder, therefore essentially radial and located in the median plane of the film.

This analysis may explain why, in electronic nanolithography, erosion begins at the entry and exit faces of α alumina, whereas it begins inside the film in the case of amorphous alumina (Humphreys et al., 1990).

The second difficulty is even harder to resolve, since the initially trapped charges may create an electric field which could deflect those incident particles arriving later, and which will be trapped in turn. The result is a time-dependent variation of the distribution of the charges, and of the field they create. This finding, makes it difficult to use Monte Carlo simulations to theoretically obtain a distribution of this type. However, Kotera et Suga (1988) have made such a study based on the assumption that the first charges deposited were stationary, and that later charges had no effect on initial distribution and resulting field. In spite of such simplifying assumptions, this type of calculation has the merit of showing qualitatively the amplitude of deflections caused by the electric field, which, if disregarded, introduce errors in the quantitative

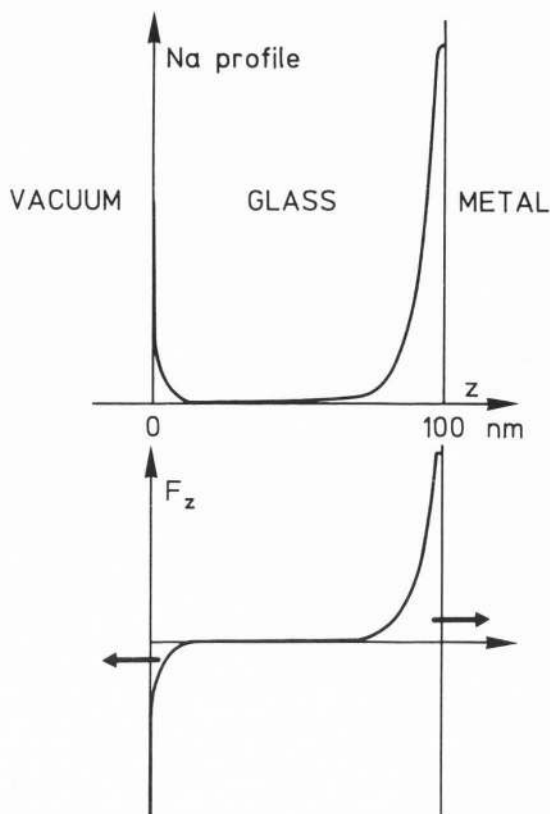


Figure 6 : Comparison between the experimental profile of sodium obtained with a vacuum/glass/metal system in which the glass was irradiated with electrons (top) and the calculated change of the electric field (bottom).

analysis of mineral insulators subjected to EPMA analysis (through overestimation of the absorption correction; Cazaux, 1988).

Last, it should be noted that the pressure pulse method developed by Cals et al. (1988) permits, in some cases, the experimental determination of trapped charge distribution $\rho(z)$.

4. Change of charge with time

After irradiation (discharging)

If it has been possible to create volume charges in an insulator, the change of these charges with time (when irradiation has ceased) can be deduced by a Maxwell equation (6) from Ohm's law :

$$j = \gamma F \quad (8)$$

and conservation of the electric charge (as here, unlike in § 2, steady state conditions do not obtain) :

$$\text{div} (j + \epsilon \frac{\partial F}{\partial t}) = 0 \quad (9)$$

(where j = the conduction current density).

The following is obtained :

$$\rho(t) = \rho(0) e^{t/\tau} \quad (10)$$

when $\tau = \epsilon/\gamma$ (τ can be calculated from tabulated values of ϵ and γ).

This approach, based on general laws, would seem to be more rigorous than the frequently used assumption in which the discharge is regarded as that of a plane capacitor through a resistor.

The discharge can be extremely slow as it continues for a number of years in electrets (Cazaux, 1986b). It can be established experimentally by measuring, at one point, the potential and its change created by the charges (as, at this point, the potential will be proportional to the charges which create it). A spectacular example is given by the mirror effect (Le Gressus et al., 1984).

Change under irradiation (charging)

For the specimen to discharge, it must have already been charged. As the microscopic hypothesis of such charging are described further on, we shall consider here that the trapping is carried out at defects of which the density is N (per unit volume) with an effective capture cross section Q .

The definition of the effective capture cross section makes it possible to write the increase in density of the trapped charges ρ_c , during the unit of time, as :

$$(\partial\rho_c/\partial t) = j_0 N.Q \quad (11)$$

(where j_0 = the current density including the secondary electrons in the insulator).

During the same time interval, recombination mechanisms have canceled out :

$$\partial\rho_r/\partial t = -\rho/\tau_r \quad (12)$$

which is simply an expression analogous to that making it possible to determine expression (10) but with a time constant τ_r under irradiation.

The conservation of the electrical charge results in $(\partial\rho/\partial t) = (\partial\rho_c/\partial t) - (\partial\rho_r/\partial t)$ hence :

$$(\partial\rho/\partial t) + (\rho/\tau_r) = j_0 N.Q \quad (13)$$

which when solved gives :

$$\rho(t) = j_0.N.Q. \tau_r (1 - e^{-t/\tau_r}) \quad (14)$$

Expression (14) resembles the charging of a capacitor through a resistor and this result is substantiated by the experiments of Boiziau et al. (1984) on films of polyacrylonitrile which correspond to values of τ_r (Cazaux, 1986a) of the order of one hour.

The analysis of the results can be complicated due to the fact that the specimen changes under the electron beam (contamination, desorption of species such as oxygen) resulting in a sudden increase in the superficial conductivity (which can also be related to flashover) and a time constant τ_2 .

If this phenomenon occurs in time t_0 , calculations (in progress) show that the variation of $\rho(t)$ when $t > t_0$, obeys the following expression :

$$\rho(t) = (\rho(t_0) - j_0 N Q \tau_2) \exp(t_0 - t)/\tau_2 + j_0 N Q \tau_2 \quad (15)$$

A change shown in figure 7, which perfectly reflects the experimental results of Ichinokawa et al. (1974).

Critical analysis

To our knowledge, the above theoretical analysis is the first to have been developed for insulators; it was inspired by the approach used with semiconductors (Szé, 1985a and b; Bourgoïn and Lannoo, 1983). Unfortunately, contrary to the case of semiconductors, it suffers from a lack of experimental data on the nature of the traps, on their effective cross sections Q and on the lifetime τ_r or trapped particles.

5. Microscopic causes

What are the microscopic causes of charging effects ?

The obvious remark is that the incident electrons penetrating the insulator either have a very short dwell time there or that they do not all participate in these effects. Indeed, elementary calculation shows that if this were not the case, the electric field that they induce would reach a destructive value (10^7 V/cm) in less than a second for irradiation of the order of $j_0 = 1 \mu\text{A}/\text{mm}^2$ (Cazaux, 1986b).

Before answering the crucial question, it should also be observed that in contrast to semiconductors, there is not, to our knowledge, a complete theory which details the microscopic mechanisms in the bombardment of insulators by electrons with energies in the 1 keV to 100 keV (not enough to displace atoms) even though mention should be made of the remarkable investigations of SiO_2 by Vigouroux et al. (1985).

The reason is to be found in the lack of reliable experimental results, since experiments in this field turn out to be extremely exciting.

In the absence of these theories we will restrict ourselves to suggesting a description based on a few experimental results which appear to us to be significant.

When the beam of incident electrons enters the insulator it produces ionizations of core electronic levels (giving rise to Auger and X-ray emissions) but, especially, the breaking of valence bonds inducing the formation of electron-hole pairs.

The excited electrons can form, in their turn, electron-hole pairs or can go out of the sample (secondary emission) on the condition that they are formed close to the surface, at a depth with an order of magnitude corresponding to their escape length, d_s (see fig. 8). As, in contrast to the case of metals, the primary and secondary electrons cannot interact with the conduction electrons, this escape length will be larger than in the metals (see section 3). After having progressively lost their energy the primary

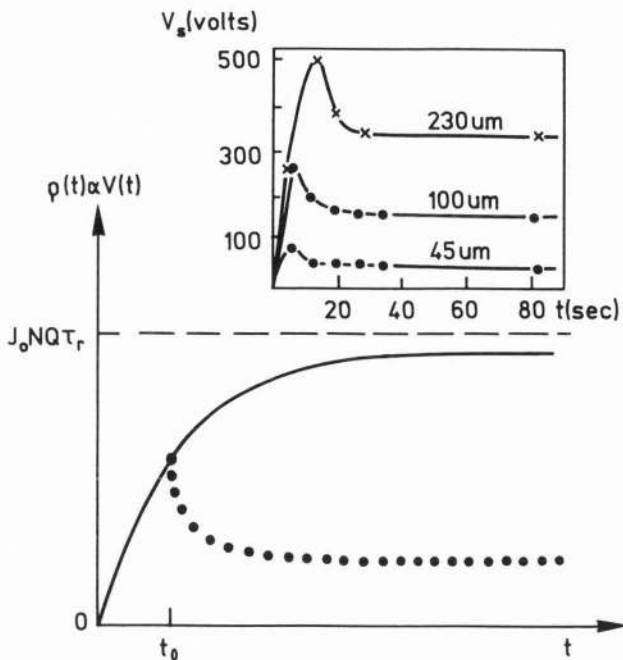


Figure 7 : The unbroken line shows the variation of trapped charge with time corresponding to expression (14). The dotted line shows the curve corresponding to expression (15) assuming modification of the conductivity from time t_0 . Experimental data obtained by Ichinokawa et al. (1974) are shown in inset.

electrons (with the exception of the backscattered electrons) will penetrate further in the solid and behave, nevertheless, as hot electrons in the conduction band. Some of these will be able to recombine with the excess holes or be trapped by defects (impurities, dislocations) in the insulator, and, in this last case, to form a negatively charged layer with a thickness d_1 . It can, therefore, be imagined that, at least during the irradiation, there is the formation of a double layer with a positive charge thickness d_2 and a negative charge thickness d_1 (Cazaux, 1986a).

At high primary energy in an insulator with numerous defect-traps, the range of incident electrons in the material can be high and the trapped negative charges will outweigh the holes left at the surface; they will induce, therefore, a negative potential. At lower primary energy the decrease of the range of electrons will reverse the sign of this potential.

The presence of defect-traps appears to be indispensable in the negative charge mechanism, otherwise, how can one answer the crucial question: where are the excess hot electrons going in the conduction band? The role of these defects has just been shown in a spectacular way by Jardin et al. (1990) who were able to fracture, by simple electron bombardment, a bent corindon crystal: the stresses on the crystal induced highly localized defects which very efficiently trapped the incident electrons, giving rise to a Coulomb repulsion that was strong enough to produce the fracture. Similarly

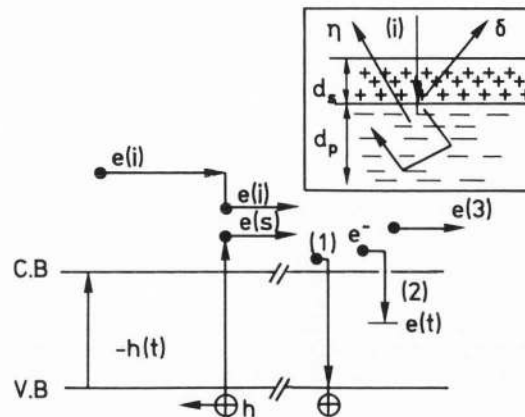


Figure 8 : Representation in a band diagram of the charging effect production mechanisms (in the absence, for simplicity, of the induced electric field). The incident electron $e(i)$ in the conduction band (C.B.) creates electron-holes pairs: $e(s)-h(s)$. The electrons can then either be recombined with holes (1) or be captured by trapped levels in the forbidden band (2) or either be directly collected by the grounded electrodes (specimen current) or emitted into the vacuum (3) -secondary electron emission-. The inset shows the same processes in actual space.

this role is also suggested in explaining (see section 3) the results in hole drilling on alumina reported by Humphreys et al. (1990). Inversely, the absence (or more exactly a limited number) of defects leads to other surprising results: for primary energies varying between 0 and 5 keV, Möeller and He (1986) did not observe any charge effect in a perfectly clean MgO crystal whereas the charge became negative when fractions of a monolayer of copper were deposited on the crystal (when it was rather expected that the charge would be positive). The hypothesis is that the copper induces traps for electrons and clean MgO cannot trap them except on the surface defects.

An insulator without defects would not be charged and the species in excess (electrons or holes) are propagated non-ohmically in the sample before. In fact, this non-ohmic current is necessary for the conservation of the current in a stationary regime, since if the total emission yield (secondary and backscattered) does not exactly balance the entering electron beam, the excess species must continue to move about in the sample, in spite of a surface potential so low as to be unmeasurable.

6. Conclusion

In this article we have attempted to review the extremely complex mechanisms relating to the effects of charges in insulators, beginning with macroscopic phenomena and ending with microscopic causes.

In view of the great diversity of the materials concerned and methods of investigation, we cannot pretend to describe or

explain everything, and we have disregarded a certain number of aspects such as the problems relating to mechanical brittleness correlated with dielectric properties (see Le Gressus et al., 1989). From the strictly electrical point of view to which we have restricted ourselves, it can be considered that the macroscopic effects are beginning to be recognized. On the other hand, the microscopic causes necessitate further experimental investigation and an in-depth theoretical approach.

The analysis of these causes is difficult but that need not make us pessimistic since what is presented is the extraordinary and fascinating field of a large part of the physics of insulators.

If these charge effects are often regarded in negative terms this should not prevent us from seeing their positive effects (electrets, metal adhesion on insulators, nanolithography, etc.) many of which have not yet been explored.

Last, this article starts with known macroscopic effects and works back to less certain microscopic causes. Logic would require reading the article in the reverse order: the charge entrapment processes (section 5) and their time variations (section 4) being well understood, it should normally be possible to calculate the electric field and the potential which they create at any point in space (by applying the laws of electrostatics -section 3-). The solutions derived should satisfy boundary conditions (continuity equations at interfaces, ground conductors at zero potential) and the laws of electrostatics (conservation of charge, conservation of current in the steady state (section 2), disregarding, if necessary, uncertain relationships such as Ohm's law.

In the present state of knowledge, this approach would be premature; it is, however, an ambitious objective for the years to come.

References

Barth G, Linder R, Bryson C (1988). Advances in charge neutralization for XPS measurements of non-conducting materials. *Surface Interface Analysis* 11, 307-311.

Battaglin G, Della Mea G, De Marchi G, Mazzoldi P, Miotello A, Guglielmi M (1982). Alkali migration in glasses on electron, proton and heavier ion irradiations. *Journal de Physique Colloque C2*, 43, 645-648.

Boiziau C, Leroy S, Perreau J, Zalczer G, Lecayon G, Le Gressus C (1984). Charge phenomena on organic materials. *Scanning Electron Microscopy 1984 III*; 1187-1192.

Bourgoin J, Lannoo M (1983). Point defects in semiconductors II. *Springer Series in Solid State Science* 34. Springer Verlag Berlin Heidelberg NY, Chap. 6, 1154-1192.

Brunner M, Schmid R (1986). Charging effects in low voltage scanning electron microscope methodology. *Scanning Electron Microscopy 1986 II*; 377-382.

Cals MP, Marque JP, Alquié C (1988). High resolution pressure pulse method for measuring spatial electron distribution in irradiated insulators. *Proceedings XIIIth Int. Symp. on Discharges and Electrical Insulators*. JM Buzzi

et A Septier Edis. Les Editions de Physique 1, 264-266.

Cazaux J (1986a). Some considerations on the electric field in insulators by electrons bombardment. *J. Appl. Phys.* 55, 1418-1430.

Cazaux J (1986b). Electrostatics of insulators charged by incident electron beams. *J. Microsc. Spectros. Electronique* 11, 293-312.

Cazaux J. (1986c). Electromigration and charging effects during Auger and XPS analysis of insulators. *Surf. and Interf. Analysis* 9, 133-134.

Cazaux J (1988). Surface potential and electric field induced by electron bombardment in insulators. *Proceedings 13th Intern. Symposium on discharges and Electrical Insulation in Vacuum*. JM Buzzi et A Septier Edis. Les Editions de Physique 2, 258-260.

Hobbs LW. (1974). Transmission electron microscopy of defects in alkali halide crystals. *Surface and Defects properties of Solids*, Vol. 4, Ed. MW Roberts and JM Thomas (The Chemical Society, London), 152-250.

Hobbs LW (1990). Murphys's law and the uncertainty of electron probes. *Scanning Microscopy Supplement* 4.

Humphreys CJ, Bullough TJ, Devenish RW, Maher DM, Turner PS (1990). Electron beam nano-etching in oxides, fluorides, metals and semiconductors. *Scanning Microscopy Supplement* 4, 185-192.

Ichinokawa T, Iiyama M, Onoguchi A, Kobayashi T (1974). Charging effect of specimen in scanning electron microscopy. *Japanese Journal of Applied Physics* 13, 1272-1277.

Jardin C, Durupt P, Robert D, Michel P, Le Gressus C (1990). Dégats d'irradiation électronique du Corindon. *Materials Science and Engineering*, B7, 119-125.

Kotera M, Suga H (1988). A simulation of keV electron scattering in a charged-up specimen. *J. Appl. Phys.* 63, 261-268.

Le Gressus C, Vigouroux JP, Duraud JP, Boiziau C, Geller J (1984). Charge neutralization on insulators by electron bombardment. *Scanning Electron Microscopy 1984 I*; 41-48.

Le Gressus C, Valin F, Gautier M, Duraud JP, Cazaux J, Okuzumi H (1989). Charging phenomena on insulating materials: mechanisms and applications. *Proceedings of the 1st European Workshop on Modern Developments and Application in Microbeam Analysis*. Editions EMAS and University of Antwerp, 151-180.

Liehr M, Thiry PA, Pireau JJ, Caudano R (1986). Characterization of insulators by high-resolution electron-energy loss spectroscopy: application of a surface potential stabilization technique. *Phys. Rev. B* 33, 5682-5697.

Möeller PJ, He JP (1986). Electron beam induced charging of Cu/MgO interface. *Nuclear Instr. and Methods in Physics Research B* 17, 137-140.

Niedrig H (1982). Electron backscattering from thin films. *J. Appl. Phys.* 53, R15-R49.

Ohuchi F, Ogino M, Holloway PH, Pantano Jr CG (1980). Electron beam effect during analysis of glass thin film with Auger Spectroscopy *Surface Interf. Anal.* 2, 85-90.

Reimer L (1985). Scanning Electron Microscopy. Springer Berlin Heidelberg, 119-127.

Schou J (1988). Secondary electron emission from solids by electron and proton bombardment. Scanning Microscopy 2, 607-632.

Szé SM (1985a). Semiconductor devices : Physics and Technology. John Wiley and Sons, NY, Chichester, Chaps. 2-4 and 2-5, 44-66.

Szé SM (1985b). Semiconductor devices. John Wiley and Sons. Chaps. 3-6, 100-107.

Tencé M, Walls MG, Jeanguillaume C, Colliex C, Thomas X, Jbara O, Cazaux J (1989). Electron irradiation effects : a tune-energy representation. Inst. Phys. Conf. Series 98, 311-314.

Vigouroux JP, Duraud JP, Le Möel A, Le Gressus C, Griscom DL (1985). Electron trapping in amorphous SiO₂ studied by charge build up under electron irradiation. J. Appl. Phys. 57, 5139-5151.

Werner HW, Warmoltz N (1984). Beam techniques for the analysis of poorly conducting materials. J. Vac. Sci. Technol. A 2, 726-731.

Whetten NR, Laponski AB (1959). Secondary Electron emission from MgO thin films. J. Appl. Phys. 30, 432-435.

Discussion with Reviewers

D. Köhler : Do you think that charging effects can be used to investigate properties of insulating or semiconducting materials ?

Authors : As shown in this article, the microscopic causes of charge effects are not fully understood, and investigations in that area must be completed before charge effects can be applied to research on the basic properties of insulators and semiconductors. As regards applications, however, the positive aspects of charge effects are beginning to be perceived and put to work, e.g., in electrets, metal/insulator bond, nanolithography. We are convinced that all these positive aspects have not, by far, been explored yet and this opens a very wide and fruitful scope for research.

D. Newbury : The idealized curve of electron emission from insulators is the basis of all discussion (fig. 1). However, the interaction of electron beams in insulators produces a dynamic situation in which the effective beam energy changes. How can we understand the true $(\eta+\delta)$ function for insulators under these dynamic conditions ?

P. Kruit : What is the effect of negative charging of insulators on the secondary electrons inside the material ? Can this effect have an influence on the secondary emission coefficient ?

Authors : The true (or ideal $(\eta+\delta)$) function would be that associated with a zero field in the insulator, since this field can obviously affect secondary emission. Further, this field is dependent on the experimental conditions specific to each experiment (location of surface with zero potential, incident probe diameter and current, etc.). This explains why experimental data on insulator secondary emission are so few (and sometimes in contradiction with one

another). To obtain the ideal curve, would therefore require extrapolating the results obtained with various field values, so as to derive the emission curve under zero field conditions.

K. Kotera : How can you take into account the thermal effect in the spectrum during electron beam bombardment ?

Authors : Our analysis does not take this effect into consideration. Naturally, the physical properties of materials can vary due to temperature effects, but such variations depend on the specific nature of the insulators investigated (there is no general law). In the broader context of irradiation effects, these temperature effects seem to have been frequently overestimated whereas those of the induced electric field have often been underestimated, or even disregarded. Even if it does not explain everything, the electric field seems to be, in Humphrey's experiments, more of a determining factor than the temperature rise. Further, it should be pointed out that temperature should not significantly alter the density of intrinsic charge carrier in the insulator ($n_i \propto \exp(-E_g/2kT)$) because their forbidden band E_g is too large ($E_g \geq 5$ eV).

L.W. Hobbs : It is well known that in electron microscopy of bare insulators catastrophic electric discharge breakdown can occur. Before discharge occurs, there exists a regime of non-ohmic conduction which constitutes a leakage current which must be included in the overall charge balance which determines the potential. Have you considered this term as well ?

M. Kotera : When the electric field becomes very high in the specimen, you will see the effect of tunneling. How can you treat that ?

Authors : First of all, it should be stressed that only those electrons (and holes), whether extrinsic or intrinsic, pre-existent in the conduction (valency) band of the insulator prior to irradiation, can exhibit ohmic behaviour ; their density, however, is negligible. In contrast, incident, beam electrons do not show ohmic behaviour in a vacuum ; why should they as soon as they enter the insulator ? This is equivalent to emphasizing the fact that, in the case of electrons injected into the insulator, non-ohmic behaviour should be the rule rather than the exception. As regards the dielectric breakdown process, the major problem is to determine whether it is the same as the breakdown process of insulators subjected to an electrostatic field or rather if incident bombardment play a decisive role in initiating the breakdown. The process illustrated by figure 9 favours this second cause.